Article

Evaluating Eco-Friendly Refrigerant Alternatives for Cascade Refrigeration Systems: A Thermoeconomic Analysis

G. Shanmugasundar [1,*] , Kamaraj Logesh [2], Robert Čep [3,*] and Ranendra Roy [4]

[1]   Department of Mechanical Engineering, Sri Sairam Institute of Technology, Chennai 600 044, India
[2]   Department of Mechanical Engineering, Vel Tech Rangarajan Dr. Sagunthala R&D Institute of Science and Technology, Avadi 600 062, India; klogesh@veltech.edu.in
[3]   Department of Machining, Assembly and Engineering Metrology, Faculty of Mechanical Engineering, VSB-Technical University of Ostrava, 708 00 Ostrava, Czech Republic
[4]   Department of Automobile Engineering, Dr. Sudhir Chandra Sur Institute of Technology and Sports Complex, Kolkata 700 074, India; ranendraroy2009@gmail.com
*   Correspondence: shanmugasundar.mech@sairamit.edu.in (G.S.); robert.cep@vsb.cz (R.Č.)

Abstract: A simple vapor-compression refrigeration system becomes ineffective and inefficient as it consumes a huge energy supply when operating between large temperature differences. Moreover, the recent Kigali amendment has raised a concern about phasing out some hydrofluorocarbon refrigerants due to their impact on the environment. In this paper, a numerical investigation is carried out to compare the performance of a cascade refrigeration system with two environmentally friendly refrigerant combinations, namely, R170–R404A and R41–R404A. Refrigerant R170, from the hydrocarbon category, and refrigerant R41, from the hydrofluorocarbon category, are separately chosen for the low-temperature circuit due to their similar thermophysical properties. On the other hand, refrigerant R404A is selected for the high-temperature circuit. An attempt is made to replace refrigerant R41 with refrigerant R170 as a possible alternative. The condenser temperature is kept constant at 40 °C, and the evaporator temperature is varied from −60 °C to −30 °C. The mathematical model developed for the cascade refrigeration system is solved using Engineering Equation Solver (EES). The effect of evaporator temperature on different performance parameters such as the COP, exergetic efficiency, and total plant cost rate is evaluated. The predicted results show that the thermoeconomic performance of the R170–R404A-based system is marginally lower compared to that of the R41–R404A-based system. The system using refrigerant pair R170–R404A has achieved only a 2.4% lower exergetic efficiency compared to the system using R41–R404A, with an increase in the annual plant cost rate of only USD 200. As the global warming potential (GWP) of R170 is less than that of R41, and R170 belongs to the hydrocarbon category, the use of the R170–R404A combination in a cascade refrigeration system can be recommended as an alternative to R41–R404A.

Keywords: cascade refrigeration system; R170; co-efficient of performance; exergetic efficiency; annual plant cost

1. Introduction

A huge amount of energy is required for refrigeration and air conditioning purposes in hotter climatic regions where the temperature difference between the evaporator and the condenser is high. The International Institute of Refrigeration recently reported that nearly 17% of the total energy used worldwide is utilized for refrigeration [1]. In such a case, the compressor power requirement increases, while the cooling effect decreases. Consequently, the system needs to run for a longer time, which can result in a breakdown of the system. This problem of operating a system having a high-temperature lift can be solved by employing a cascade refrigeration system (CRS). On the other hand, [2] recommended phasing out the production and consumption of high-GWP HFC refrigerants. Hydrocarbons have lower GWP and zero ODP. So, these substances can be considered as

alternative refrigerants for long-term purposes, if they can provide satisfactory performance in a CRS.

Different researchers have made numerous studies on CRSs. Lee et al. [3] performed a thermodynamic analysis on a CRS using the R744–R717 refrigerant combination to determine the optimal condensing temperature (T_{cond}) in a cascade condenser (CC) to maximize the COP and minimize the exergy loss. They noted a rise in the optimal condensing temperature of the cascade condenser (T_{LC}) with T_{cond}, T_{eva}, and ΔT. Hoşöz [4] carried out a comparative experimental study between two refrigeration system configurations: single stage and a CRS using R134a as the refrigerant. The author noted a COP of 3.5 and 1.5 for the single-stage VCR and CRS, respectively, while keeping the refrigeration capacity fixed at 500 W. Nicola et al. [5] carried out a simulation to evaluate the performance of a CRS using ammonia as the high-temperature refrigerant, blends of carbon dioxide, and four different HFCs, namely, R23, R41, R125, and R32, as low-temperature refrigerants. They concluded that the use of the HFC/carbon dioxide blends for low-temperature applications could be an attractive option. Niu and Zhang [6] experimented on a CRS using blend of R290 and R744 in the low-temperature circuit (LTC) to replace R13 and R290 in the high-temperature cycle. They noted a higher COP and refrigeration effect with the new mixture compared to those using R13 as refrigerant. Ouadha et al. [7] performed a comparison between CRS and two-stage refrigeration using natural refrigerants, namely, carbon dioxide (R744), ammonia (R717), and propane (R290). They observed slightly lower power consumption in the low-pressure compressor of the cascade system compared to the two-stage system. However, nearly 13% higher power consumption was noted in the high-temperature compressor of the cascade system compared to that of the two-stage system. Sun et al. [8] used two refrigerant combinations in their numerical work on a CRS and found better performance using the R41–R404A refrigerant pair. They noted the maximum exergetic efficiencies of the R41/R404A and R23/R404A CRSs to be 44.38% and 42.98%, respectively. Dopazo and Fernández-Seara [9] also experimentally investigated a CRS with the natural refrigerant combination R744–R717 to determine the optimal condenser temperature of the low-temperature circuit condenser. Dopazo et al. [10] theoretically simulated a CRS using natural refrigerant pair R744–R717 and experienced a decrease in the COP with the increase in T_{cond} and ΔT. They also mentioned that the use of carbon dioxide was advantageous, as it reduced the flammability of the hydrocarbons. Rezayan and Behbahaninia [11] conducted thermoeconomic optimization on a CRS using CO_2–NH_3. They investigated the effect of different operational parameters on the system cost rates. They noted the optimum annualized cost of the system to be USD 109242, which was 9.34% lower than the cost of the base case system. Colorado et al. [12] carried out a thermodynamic analysis of a CRS for simultaneous cooling and heating using ammonia (NH_3), R134a, butane, and propane in the low-temperature cycle (LTC) and carbon dioxide (CO_2) in the high-temperature cycle (HTC) as refrigerants to find out the optimum performance and optimum design parameters. They found up to 7.3% improvement in the COP using butane in the LTC compared to that with NH_3–CO_2. Messineo and Panno [13] performed a thermodynamic analysis of a two-stage CRS to replace synthetic refrigerants with natural refrigerants. They obtained a maximum COP of 1.71 using natural refrigerant pair R744–R717 at evaporator and condenser temperatures of −35 °C and 35 °C, respectively. Aminyavari et al. [14] performed thermoeconomic optimization on a 50 kW cooling capacity CRS. They observed that a 24% increase in exergetic efficiency led to a 164% increase in the total cost rate. Ust and Karakurt [15] performed an exergetic analysis of a CRS using different refrigerant couples, namely, R23–R290, R23–R404A, R23–R507A, and R23–R717. They noted a decrease in the rate of exergy destruction with the increase in T_{eva} and a rise in the rate of exergy destruction with the rise in T_{cond} and ΔT. Kasi [16] carried out a numerical analysis to analyze the energetic performance of a CRS separately using R-23, R508B, and R170 in the LTC and R134a, R290, R404A, R407C, and R410A in the LTC. They observed the best performances using refrigerant pair R170–R134a and worst performances using refrigerant pair R404A–R508B among all the investigated refrigerant pairs. Rawat and

Pratihar [17] thermodynamically analyzed a CRS using N_2O in the LTC and five different refrigerants, namely, R717, R290, R1290, R134a, and an azeotropic mixture R507A in the HTC. Gholamian et al. [18] exergetically simulated a CO_2/NH_3-based CRS to determine the magnitude and location of the exergy destructions. The authors of the study determined through a conventional exergy analysis that the condenser of the NH_3 cycle, as well as the throttling valve and compressor of the CO_2 cycle, experienced the most significant exergy destruction. However, the results of an advanced exergy analysis indicated that improvements were needed in the throttling valve, compressor, and cascade condenser of the CO_2 cycle. In fact, the authors found that improving the performances of these components could yield a 63% improved cycle performance. Patel et al. [19] performed a comparative thermoeconomic analysis and optimization of a CRS using refrigerant pairs NH_3/CO_2 and C_3H_8/CO_2. They concluded that the C_3H_8/CO_2 pair offered 5.33% less cost with 6.42% more exergy destruction compared to the NH_3/CO_2 pair. Roy and Mandal [20] presented a numerical investigation on a CRS and recommended R161 as an alternative to R404A in the high-temperature cycle. Adebayo et al. [21] performed a comparative thermodynamic analysis on a CRS using CO_2 in the LTC and four different refrigerants, namely, NH_3, R717, HFE7000, and HFE7100 in the HTC. Aktemur and Öztürk [22] thermodynamically simulated a CRS using low GWP refrigerant R41 in the LTC and R1243zf, R423A, R601, R601A, R1233zd (E), and RE170 in the HTC. They noted the worst performances in terms of COP and exergy efficiency using R41–R423A. On the other hand, they noted the maximum COP and exergy efficiency to be 1.210 and 37.18%, respectively, using R41–RE170. In another study, Aktemur et al. [23] studied the effect of T_{eva}, T_{cond}, and ΔT on the system's thermodynamic performances using three low-GWP refrigerant pairs, namely, R41–R601, R41-cyclopentane, and R41–R602A. They noted the best thermodynamic performances using R41–R601, which exerted maximum exergetic efficiencies of 43.10%. However, they noted a very high compressors' discharge temperature over 120 °C for all three refrigerant pairs. Zhang et al. [24] conducted an experimental investigation on a CRS using $R1270/CO_2$ as the refrigerant combination and noted a rise in the COP and cooling capacity with the increase in T_{HE}. Chen et al. [25] investigated the influence of the subcooling degree in the LTC of a NH_3/CO_2 CRS to find out the thermodynamic performances of the system. They reported 4.58% improvement in the COP and 4.4% improvement in the exergy efficiency of the modified system compared to the conventional CRS when the subcooling degree was kept fixed to 10 °C. Sun and Wang [26] simulated a modified CRS for industrial application using the R1150/R717 refrigerant pair to replace the three-stage CRS using R1150/R41/R717 as the refrigerant combinations. Faruque et al. [27] simulated a CRS using Trans-2-butane, Toluene, Cyclopentane, and Cis-2-butane as refrigerants and thermodynamically analyzed the system. They noted the maximum COP and exergy efficiency using the Trans-2-butane/Toluene refrigerant combination. Cabello et al. [28] experimentally analyzed the energy performance of a CRS using four alternative refrigerant pairs, namely, R290/R744, R1270/R744, R600a/R744, and R1234ze(E)/R744 and compared the results with the system using R134a/R744. They also carried out an environmental analysis and noted less CO_2 emission using all four refrigerant pairs. Deymi-Dashtebayaz et al. [29] presented an energy–exergoeconomic–environmental analysis on a CRS using six pairs of low-GWP refrigerants including R41–R161, R41–R1234yf, R41–R1234ze, R744–R161, R744–R1234yf, and R744–R1234ze and reported R41–R161 and R41–R1234ze as the best refrigerant pairs in terms of the COP/exergy efficiency and total cost rate, respectively. Soni et al. [30] used CO_2 as a high-temperature cycle refrigerant and used different low-temperature refrigerants for the low-temperature cycle for the simulation of a CRS for ultra-low-temperature applications.

Despite the fact that there is a sizable amount of research works on CRSs in the literature, there is a lack of work related to today's requirements. To protect further environmental damage, the refrigerants used in systems must have a very low GWP. The phasing out of high-GWP HFC substances in refrigeration systems was suggested in the recent Kigali amendment in 2016. Moreover, the majority of published works

concentrated on CO_2-NH_3 as a refrigerant pair. Therefore, it will certainly be compelling to analyze a CRS using low-GWP refrigerant pairs of hydrocarbons. The use of hydrocarbon refrigerants will solve the environmental issues of ozone depletion and global warming caused by refrigeration and air conditioning systems. In this paper, the thermoeconomic performance of a CRS was analyzed and compared, using R170–R404A and R41–R404A as refrigerant combinations to find out a possible alternative of R41. A mathematical model was developed in Engineering Equation Solver (EES) [31] software using different energy-, exergy-, and economy-based equations to carry out the simulation work.

2. System Description

The schematic, a P-h diagram, and a T-s diagram of the CRS are shown in Figure 1a–c, respectively.
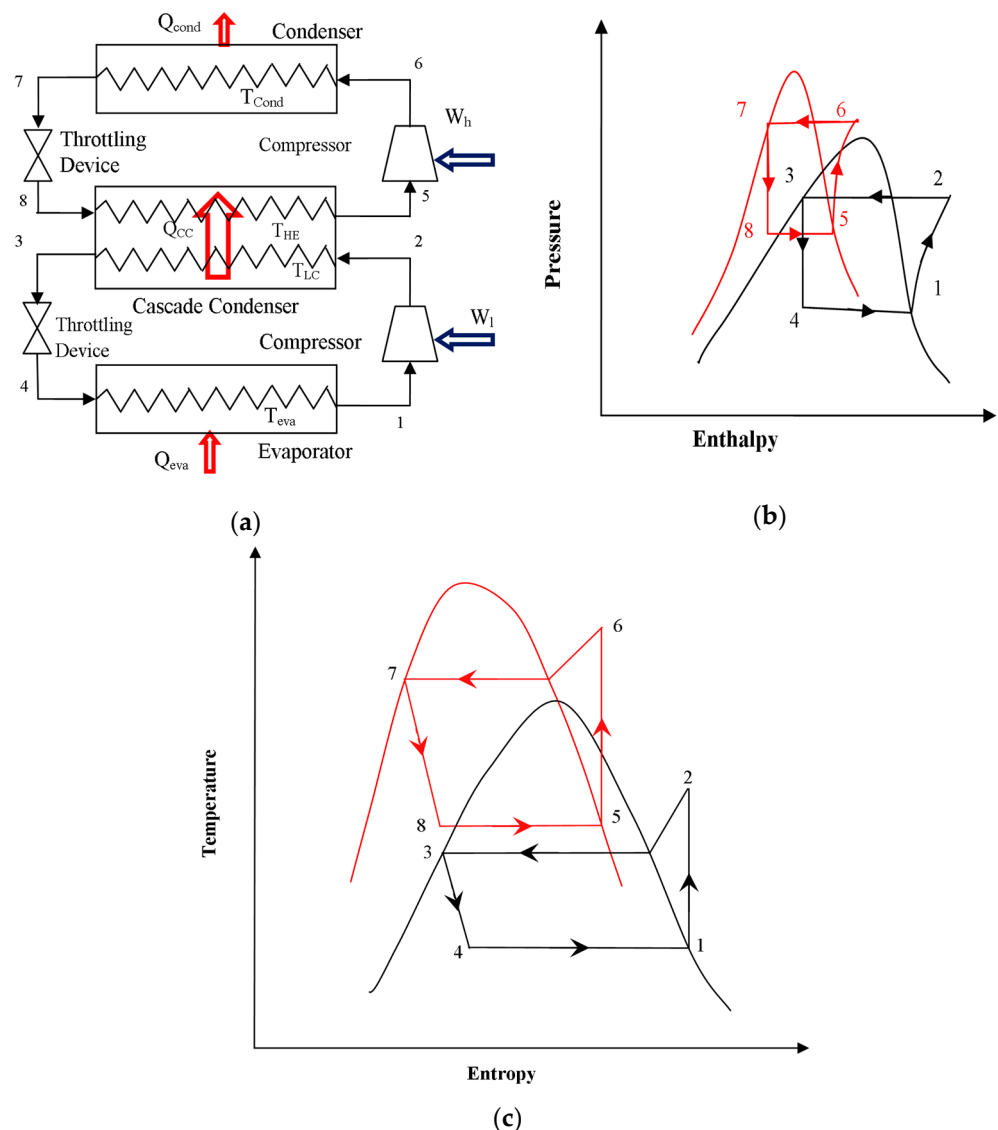

Figure 1. (**a**) Schematic diagram, (**b**) P-h diagram, and (**c**) T-s diagram of cascade refrigeration system.

The whole system consists of two basic vapor-compression refrigeration (VCR) cycles, a low-temperature circuit (LTC), and a high-temperature circuit (HTC) connected in series through a cascade condenser (CC). The CC acts as the condenser for the LTC and as the evaporator for the HTC. Refrigerant R404A is taken for the HTC, as a common refrigerant, whereas R41 and R170 are separately taken as the refrigerants in the LTC. The different

thermophysical and environmental properties of these three investigated refrigerants were taken from the work of [32], and these are presented in Table 1.

Table 1. Thermophysical properties of R41, R161, and R170 [32].

Refrigerant	Molecular Mass (gm/mole)	Critical Temperature (°C)	Boiling Point (°C)	ASHARAE Safety Code	ODP	GWP
R170	30.07	32.2	−88.9	A3	0	20
R41	34.03	44.1	−78.1	A2	0	97
R404A	97.6	72.1	−46.6	A1	0	3800

The LTC refrigerant in the evaporator absorbs Q_{eva} quantity of heat at T_{eva} and evaporates it. While entering the LTC compressor, the vapor refrigerant receives the W_l to increase its temperature and pressure. When it reaches the cascade heat exchanger, the LTC refrigerant rejects heat Q_{cc} at T_{LC}, which is subsequently absorbed by the HTC refrigerant at T_{HE}. As a result, the HTC refrigerant evaporates, and the LTC refrigerant condenses. The liquid refrigerant then enters the throttle valve and expands to the evaporator pressure. The cascade heat exchanger releases the vaporized HTC refrigerant, which again enters the HTC compressor. The HTC refrigerant is then passed to the condenser after being compressed by the HTC compressor to the condenser pressure, which requires W_h amount of work. At T_{cond}, heat Q_{cond} is rejected by the HTC refrigerant and becomes condensed. The condensed HTC refrigerant is then entered into the HTC throttle device and becomes expanded to the HTC evaporator. The important parameters that have a significant impact on CRS performance are T_{eva}, T_{cond}, T_{LC}, and ΔT.

3. Mathematical Model

The entire CRS is modeled, taking into account all of the individual processes. However, in order to reduce complexity and make the analysis feasible, pressure drops and heat losses in the pipeline are completely disregarded. Subcooling is not considered in the LTC or HTC. Superheating is taken as effective heating. All of the components are in steady-state operation. In the cascade heat exchanger, the temperature difference between the hot and cold fluids is assumed to be 5 °C. The values of some other input parameters are assumed for the analysis and presented in Table 2.

Table 2. Basic assumptions for the simulation.

Parameters	Values	Ref.
Cooling load, Q_{eva}	10 kW	
LTC compressor isentropic efficiency, $\eta_{C,l}$	80%	[33]
HTC compressor isentropic efficiency, $\eta_{C,h}$	80%	[33]
Condenser temperature, T_{cond}	40 °C	[8]
Dead-state temperature, T_0	25 °C	[34]
Evaporator temperature, T_{eva}	−60 °C to −30 °C	[8]
Superheating in the LTC and HTC	5 °C	[8]
U_{eva}	0.03 kW m^{-2} K^{-1}	[35]
U_{cond}	0.04 kW m^{-2} K^{-1}	[35]
U_{cc}	1 kW m^{-2} K^{-1}	[35]
Temperature of the inlet air to the evaporator	−10 °C	
Maintenance factor, ε	1.06	[36]
Interest rate, i	14%	[36]
Plant life time, n	15 years	[36]
Annual operational hour, N	4266 h	[37]
Electrical power cost,	0.09 USD/kWh	[38]
Emission factor, μ_{CO_2e}	0.968 kg/kWh	[39]
Cost of CO_2 avoided, C_{CO_2}	0.09 USD/kg of CO_2 emission	[38]

3.1. Energy Analysis

According to the first law of thermodynamics, the LTC mass flow rate can be calculated as follows [40]:

$$\dot{m}_l = \frac{Q_{eva}}{h_1 - h_4} \tag{1}$$

The compressor power in the LTC can be written as

$$W_l = \frac{\dot{m}_l(h_2 - h_1)}{\eta_{C,l}} \tag{2}$$

where $\eta_{C,l}$ is the LTC compressor's isentropic efficiency.

Similarly, the mass flow rate can be calculated as

$$\dot{m}_h = \frac{Q_{CC}}{h_5 - h_8} \tag{3}$$

The compressor power can be written as

$$W_h = \frac{\dot{m}_h(h_6 - h_5)}{\eta_{C,h}} \tag{4}$$

where $\eta_{C,h}$ is the compressor isentropic efficiency in the HTC.

The total compressor power requirement is given by

$$W_T = W_l + W_h \tag{5}$$

The heat load in the condenser is calculated as

$$Q_{cond} = \dot{m}_h(h_6 - h_7) \tag{6}$$

The *COP* is given by

$$COP = \frac{Q_{eva}}{W_T} \tag{7}$$

The heat transfer area of the evaporator, condenser, and cascade condenser can be expressed, following Roy and Mandal [41], as

$$A = \frac{Q}{U \times \text{LMTD}} \tag{8}$$

where U is the overall heat transfer co-efficient of the heat exchanger, and LMTD is the logarithmic mean temperature difference between the refrigerants in the heat exchangers.

3.2. Exergy Analysis

The exergy loss in an individual component of the system can be calculated using the generalized equation of exergy loss, following Arora and Kaushik [34]. This equation, Equation 9, was used to calculate the exergy loss in the different components of the system, which are mentioned in Table 3.

$$\sum ED = \sum EX_{in} - \sum EX_{out} + \sum Q\left(1 - \frac{T_0}{T}\right)_{in} - \sum Q\left(1 - \frac{T_0}{T}\right)_{out} \pm \dot{W} \tag{9}$$

Table 3. Exergy destruction function for the system components.

Components	
Evaporator	$ED_{eva} = EX_4 - EX_1 + Q_{eva} \times \left(1 - \frac{T_0}{T_{ref}}\right)$
LTC compressor	$ED_{comp,l} = EX_1 - EX_2 + W_l$
LTC expansion device	$ED_{exp,l} = EX_3 - EX_4$
HTC compressor	$ED_{comp,h} = EX_5 - EX_6 + W_h$
HTC expansion device	$ED_{exp,h} = EX_7 - EX_8$
Cascade condenser	$ED_{cc} = EX_2 + EX_8 - EX_3 - EX_5$
Condenser	$ED_{cond} = EX_6 - EX_7$

The total exergy destruction can be written as

$$ED_T = ED_{eva} + ED_{comp,l} + ED_{exp,l} + ED_{comp,h} + ED_{exp,h} + ED_{cc} + ED_{cond} \tag{10}$$

The percentage of exergy destruction in the individual components of the system is given by

$$\delta_{component} = \frac{ED_{component}}{ED_T} \tag{11}$$

The system's exergetic efficiency can be expressed as [42]

$$\eta_{ex} = \frac{W_T - ED_T}{W_T} \tag{12}$$

3.3. Economic Analysis

The total cost rate of the CRS is given by [41]

$$\dot{C}_T = \sum_k \dot{C}_k + \dot{C}_{OP} + \dot{C}_{env} \tag{13}$$

The capital cost of each individual component is estimated based on their cost functions, which are listed in Table 4.

Table 4. Capital cost components of different components of the cascade refrigeration system [34].

Components	Cost Functions
Evaporator	$C_{eva} = 1397 \times A_{eva}^{0.89}$
LTC compressor	$C_{comp,l} = 10167.5 \times W_l^{0.46}$
Cascade condenser	$C_{cc} = 383.5 \times A_{cc}^{0.65}$
LTC throttle valve	$C_{exp,l} = 114.5 \times \dot{m}_{LTC} - 4$
HTC compressor	$C_{comp,h} = 9624.2 \times W_h^{0.46}$
Condenser	$C_{cond} = 1397 \times A_{cond}^{0.89}$
HTC throttle valve	$C_{exp,h} = 114.5 \times \dot{m}_{HTC}$

The rate of capital investment and maintenance cost can be estimated as

$$\dot{C}_k = C_k \times \varepsilon \times CRF \tag{14}$$

The *CRF* can again be expressed as

$$CRF = \frac{i(i+1)^n}{(1+i)^n - 1} \tag{15}$$

where *i* and *n* are the annual interest rate and system life time, respectively.

The total capital investment and maintenance cost of the whole system can be calculated by

$$\sum_k \dot{C}_k = \dot{C}_{eva} + \dot{C}_{cond} + \dot{C}_{cc} + \dot{C}_{comp,l} + \dot{C}_{comp,h} + \dot{C}_{exp,h} + \dot{C}_{exp,l} \tag{16}$$

The operational cost of the system can be expressed as

$$\dot{C}_{OP} = N \times W_T \times \alpha \tag{17}$$

where N is the annual operational hour in hours, W_T is the total compressor power, and α is the unit electrical cost in USD/kWh.

The rate of penalty cost can be determined as

$$\dot{C}_{env} = m_{CO_2e} \times C_{CO_2} \tag{18}$$

where C_{CO_2} is the cost of CO_2 avoided, and m_{CO_2e} is the amount of annual GHG emission from the system and can be calculated as [39]

$$m_{CO_2e} = \mu_{CO_2e} \times E_{annual} \tag{19}$$

where μ_{CO_2e} is the emission factor, and E_{annual} is the annual energy consumption in kWh.

4. Results and Discussions

The model developed for the thermoeconomic analysis of the system in EES was validated by the work of [43]. The details of the input parameters for the validation are shown in Table 5.

Table 5. Details of input parameters [43].

Parameters	Values	Parameters	Values
T_{eva}	−26 °C	T_{cond}	32 °C
T_{LC}	−9 °C	T_{HE}	−11 °C
Degree of superheating in the LTC	7 °C	Degree of superheating in the HTC	0 °C
Degree of subcooling in the LTC	0 °C	Degree of subcooling in the HTC	0 °C
$\eta_{S,LTC}$	21%	$\eta_{S,HTC}$	76%
$\eta_{m,LTC}$	93%	$\eta_{m,HTC}$	93%
$\eta_{elec,LTC}$	80%	$\eta_{elec,HTC}$	80%

The work input to the LTC compressor and the COPs in both the LTC and the HTC were validated by the work of [43] and are displayed in Table 6.

Table 6. Validation of the simulation model by the work of Sawalha et al. [43].

Parameters	Predicted Data	Experimental Data	Error
W_l	1.586	1.62	−2.1%
COP_l	1.892	1.86	+1.72%
COP_h	2.889	2.65	+9.02

The quantitative similarity between the simulated and experimental results for all three parameters is reasonable. A thermoeconomic analysis of CRS was conducted to evaluate the optimal performance of the system. The effect of T_{eva} on the COP of the system, compressor discharge temperature, exergetic efficiency, and total plant cost rate were analyzed and are presented graphically. The states of the system using the R41–R404A refrigerant pair at the base case condition are shown in Table 7.

Table 7. Conditions at the different state points of the system using refrigerant pair R41–R404A at base case condition.

State Pt	Temperature (K)	Enthalpy (kJ/kg)	Entropy (kJ/kg-K)	Exergy (kW)	Mass Flow Rate (kg/s)
1	238	539.8	2.498	4.072	
2	347	648	2.562	6.824	
3	279	215.7	1.054	7.348	0.031
4	233	215.7	1.106	6.873	
5	279	371	1.623	5.353	
6	326.2	397.9	1.64	7.991	
7	313	259.9	1.2	7.148	0.121
8	274	259.9	1.218	6.506	

4.1. Effect of T_{LC} on COP

The variations of the COP_l, COP_h, and overall COP of the system, with T_{LC} using refrigerant pair R170–R404A for a T_{eva} and T_{cond} of −30 °C and 40 °C, respectively, are presented in Figure 2.
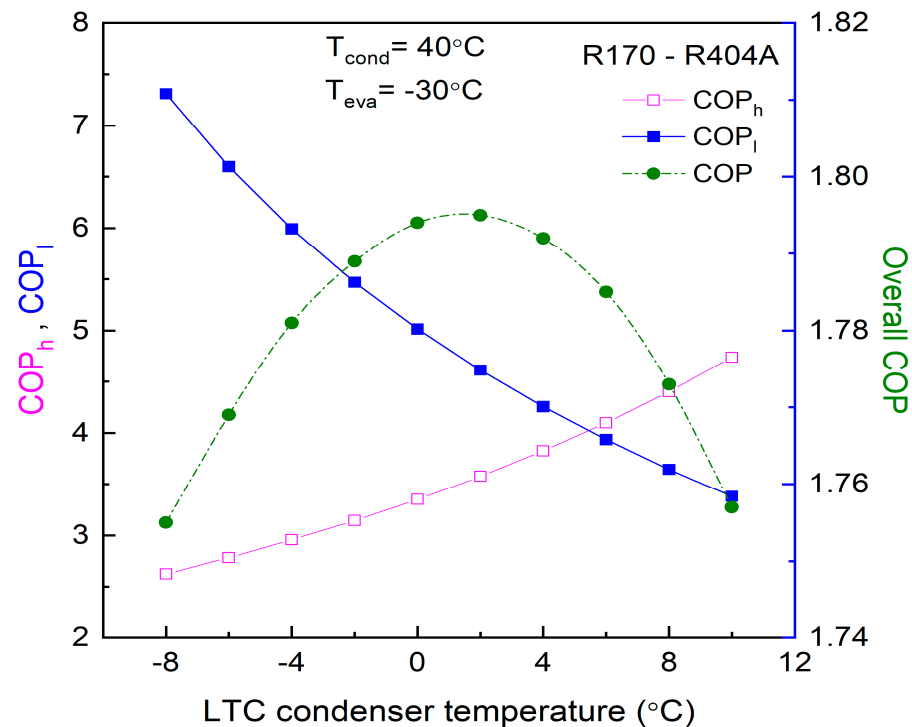
**Figure 2.** COP_l, COP_h, and overall COP vs. T_{LC}.

Figure 2 shows an initial increase with the increase in T_{LC} and reaches the peak COP. A further increase in the T_{LC} leads to a decrease in the COP of the system. The temperature lift in the LTC increases, whereas the temperature lift decreases in the HTC with the increase in T_{LC}. Consequently, the COP_l decreases, and the COP_h increases. As a result, the overall COP reaches its peak and then decreases with the increase in T_{LC}. Therefore, an optimal T_{LC} exists for any fixed T_{eva} and T_{cond} where the system gives maximum performance. It is worth noting, as shown in Figure 2, that the optimum COP is obtained at a T_{LC} of 7 °C when the T_{eva} and the T_{cond} are constant at −30 °C and 40 °C, respectively, and the value of the optimum COP is noted to be 1.845. Similarly, the optimum T_{LC} of the system was estimated while varying the T_{eva}, ranging from −60 °C to −30 °C, and the results are presented in Table 8.

Table 8. Optimum LTC temperatures for different evaporator temperatures for refrigerant pairs R170–R404A and R41–R404A.

Evaporator Temperature (°C)	R170–R404A	R41–R404A
−60	−10	−4
−55	−8	−2
−50	−6	0
−45	−4	2
−40	−2	4
−35	0	5
−30	2	6

4.2. Effect of T_{eva} on COP

Figure 3 depicts the variations of the optimal COP of the system with the T_{eva}. Figure 3 shows that the COP of the system increases with the increase in the T_{eva} for both pairs. This is attributed to the fact that as the T_{eva} increases, the pressure ratio in the LTC decreases, which results in an increase in the COP_l as well as the overall COP. The system's COP is found slightly lower when R170 is used in the LTC instead of R41. However, the differences in the COPs using R170 as the LTC refrigerant at each T_{eva} are very small compared to the differences in the COPs using R41 as the LTC refrigerant. The maximum and minimum differences were calculated, which are noted to be 2.79% and 1.85%, respectively, at a T_{eva} of −30 °C and −60 °C, respectively.
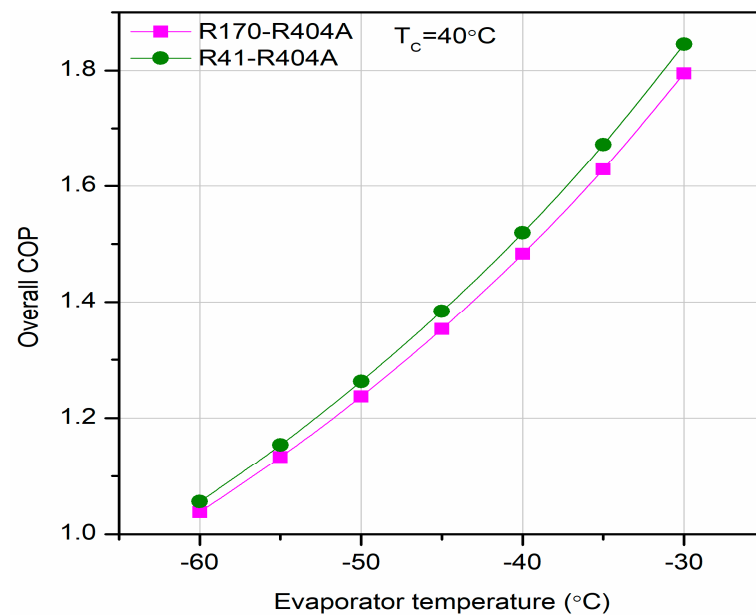
Figure 3. Optimal COP vs. T_{eva}.

4.3. Effect of T_{eva} on Compressor Discharge Temperature

The effect of the T_{eva} on the compressor discharge temperature at the optimum condition of the T_{LC} is illustrated in Figure 4 for both refrigerant pairs. Figure 4 shows that the low-temperature cycle attains a much lower compressor discharge temperature when R170 is used instead of R41, due to the lower adiabatic index of R170 compared to that of R41. The maximum compressor discharge temperature reaches 94 °C when using R41 in the system at the T_{eva} of −60 °C. However, the corresponding compressor discharge temperature when using R170 as the low-temperature cycle refrigerant is noted to be 36 °C. On the other hand, no significant changes in the compressor discharge temperatures in the high-temperature cycle (HTC) were noted, as shown in Table 9.
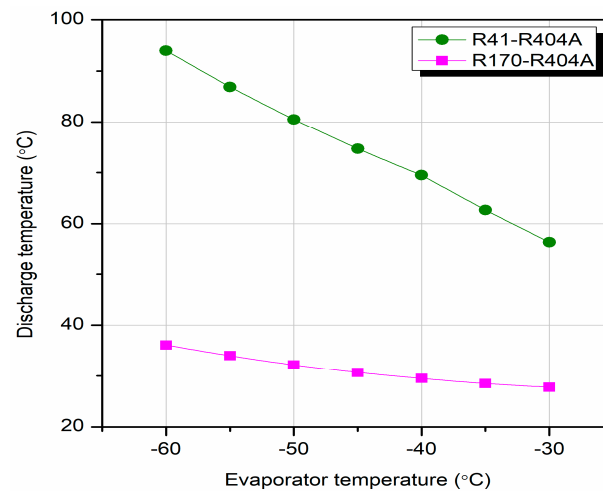
Figure 4. Evaporator temperature vs. LTC compressor discharge temperature.

Table 9. Compressor discharge temperature in the HTC for refrigerant pairs R170–R404A and R41–R404A.

Evaporator Temperature (°C)	R170–R404A (°C)	R41–R404A (°C)
−60	57.1	55.4
−55	56.5	54.9
−50	56	54.4
−45	55.4	53.9
−40	54.9	53.4
−35	54.4	53.2
−30	53.9	52.9

4.4. Effect of T_{eva} on Exergetic Efficiency

The optimum exergetic efficiency (EE) of both the R170–R404A and R41–R404A systems was compared for varying T_{eva}, which are presented in Figure 5. Figure 5 shows that the exergetic efficiency initially increases with the increase in T_{eva}, and, after reaching the peak value, it starts decreasing. Figure 5 also shows a slightly lower exergetic efficiency using refrigerant R170 in the LTC compared to using R41 as the refrigerant. The maximum exergetic efficiency is obtained at a T_{eva} of −50 °C for both systems, which is found to be 42.72% and 41.89% for the R41–R404A and R170–R404A systems, respectively.
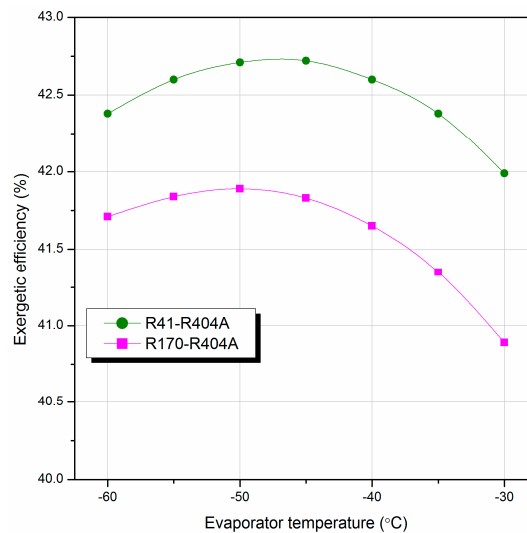

Figure 5. Evaporator temperature vs. exergetic efficiency.

The exergy destruction in the individual components of the system was separately evaluated for the two systems at different T_{eva}, corresponding to the optimum T_{LC}. The percentages of the total exergy destruction in the individual components at a condenser temperature of 40 °C are presented in Table 10.

Table 10. Proportion of exergy losses in different parts of the system.

Exergy Loss Percentage		T_{eva} °C						
		−60	−55	−50	−45	−40	−35	−30
$\delta_{Comp,l}$	R170–R404A	14.06	14.08	14.05	13.96	13.80	13.56	13.25
	R41–R404A	14.05	14.34	14.58	14.76	14.87	14.55	14.08
$\delta_{evap,l}$	R170–R404A	0.12	0.15	0.18	0.22	0.27	0.33	0.40
	R41–R404A	0.17	0.21	0.25	0.28	0.31	0.32	0.33
$\delta_{exp,l}$	R170–R404A	14.10	13.73	13.33	12.90	12.44	11.94	11.40
	R41–R404A	12.38	12.17	11.93	11.66	11.37	10.44	9.47
$\delta_{Comp,h}$	R170–R404A	18.24	18.37	18.50	18.61	18.72	18.81	18.89
	R41–R404A	16.41	16.49	16.56	16.60	16.63	17.11	17.61
$\delta_{exp,h}$	R170–R404A	24.87	24.36	23.83	23.29	22.72	22.13	21.53
	R41–R404A	20.52	20.02	19.48	18.93	18.35	18.56	18.79
$\delta_{cond,h}$	R170–R404A	18.41	19.23	20.11	21.05	22.07	23.17	24.36
	R41–R404A	18.55	19.44	20.39	21.41	22.51	23.75	25.09
δ_{cc}	R170–R404A	10.21	10.08	10.00	9.97	9.99	10.06	10.17
	R41–R404A	17.91	17.33	16.81	16.36	15.96	15.26	14.63

Table 10 clearly shows different exergy destructions in the different components of the system for the two investigated refrigerant pairs. Table 10 also shows that the least exergy is being destructed in the evaporator for both systems. On the other hand, the highest percentage of exergy is being destructed in the throttle valves of the system. A closer look at Table 10 reveals that nearly 35% of the exergy is only destructed in both the throttle valves, followed by the compressors and cascade condenser. A comparison of the percentages of exergy destruction in the individual components of the system for both the refrigerant pairs is shown in Figure 6 for a T_{eva} and T_{cond} that are fixed at −60 °C and 40 °C, respectively.
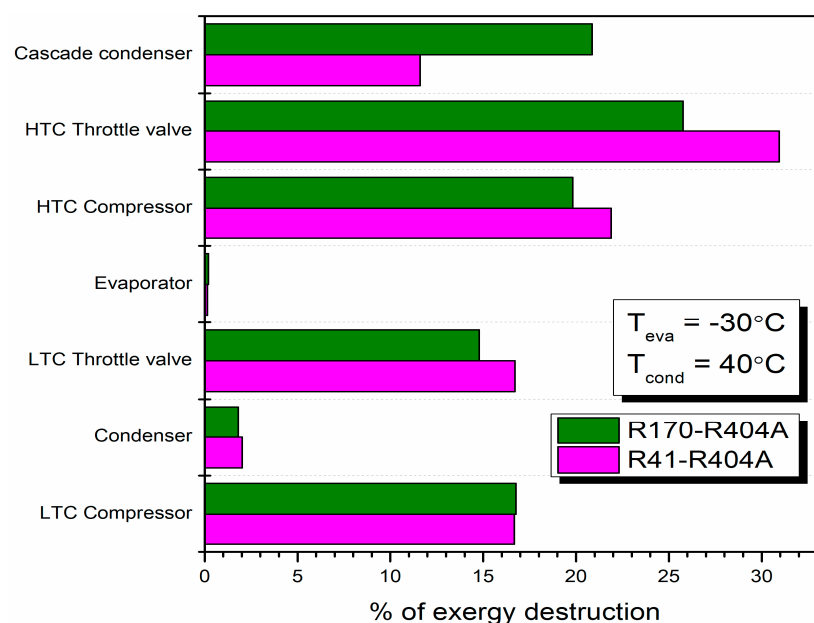

Figure 6. Component-wise exergy destruction (%).

4.5. Effect of T_{eva} on Plant Cost Rate

The variations of the plant cost rates of the R41–R404A and R170–R404A systems as a function of T_{eva} for the corresponding optimal conditions are illustrated in Figure 7.
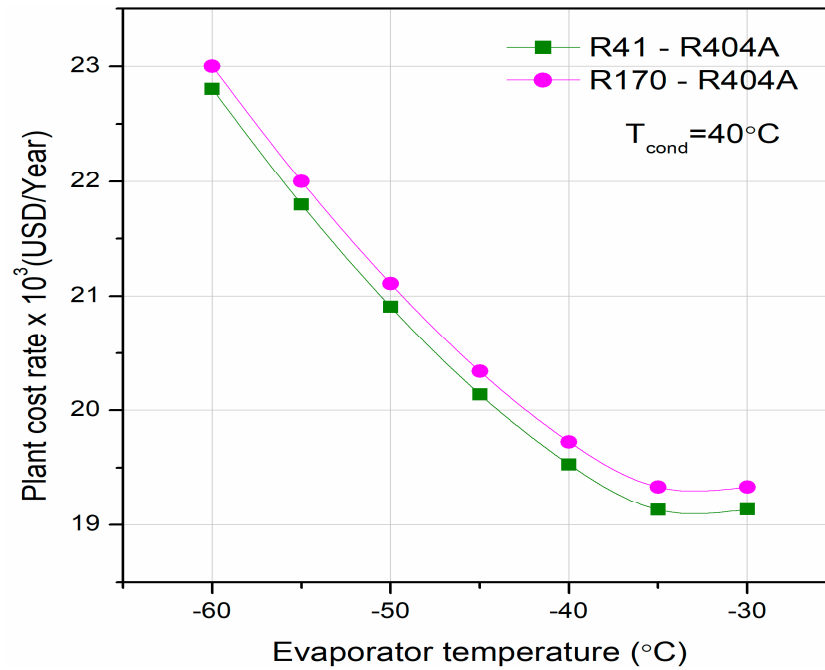

Figure 7. Total plant cost rate vs. T_{eva}.

The C_T decreases with the increase in the T_{eva} up to $-35\,°C$ and then increases with the increase in T_{eva}, as is apparent from Figure 7. Both refrigerant pairs investigated for the study show a similar trend. This is because as the T_{eva} increases, both the C_{OP} and C_{env} decrease due to the decrease in W_T, as shown in Figures 8 and 9, respectively.
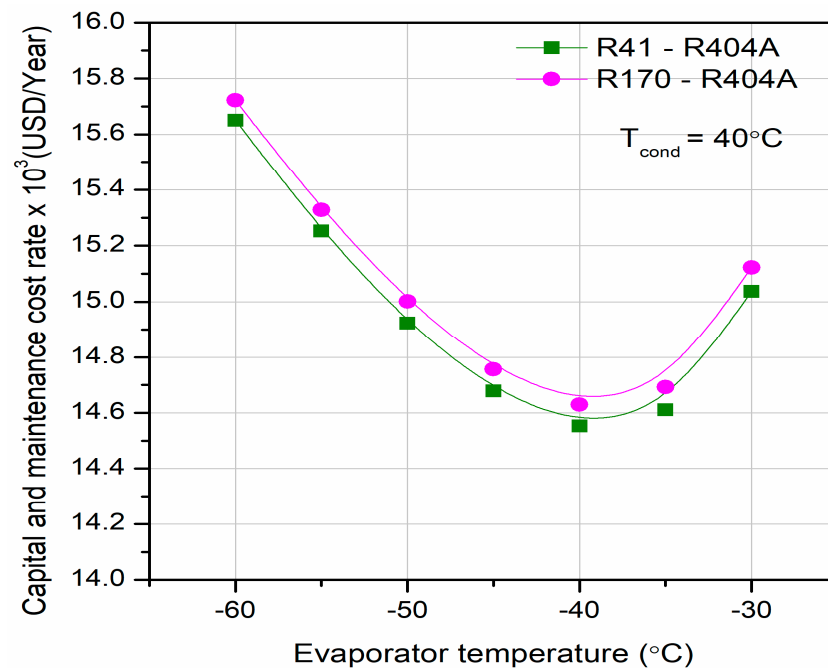
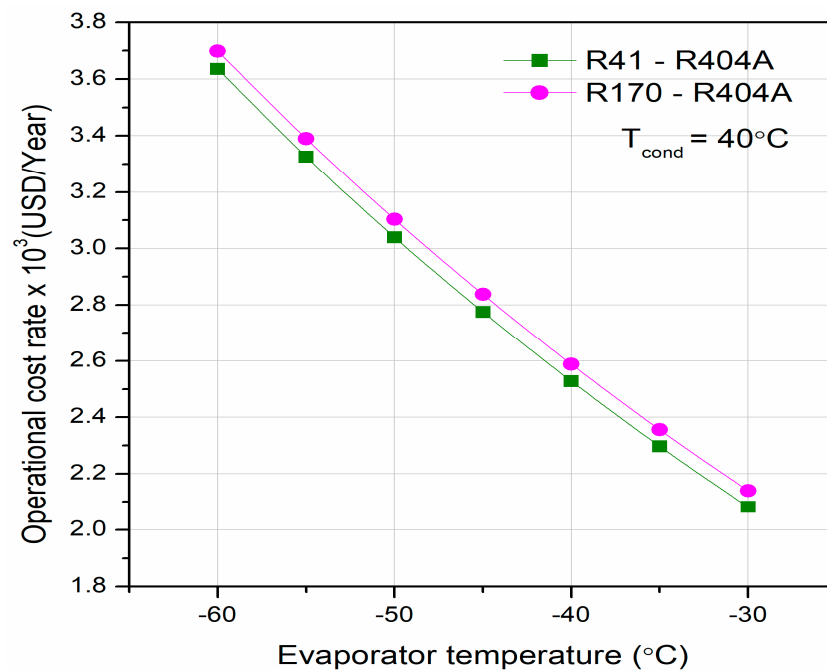**Figure 8.** Capital and maintenance cost rate vs. T_{eva}.

Figure 9. Operational cost rate vs. T_{eva}.

However, the C_T initially decreases with the T_{eva} and, after reaching the least value, it starts increasing at a much higher rate compared to the other two cost functions, as shown in Figure 10.
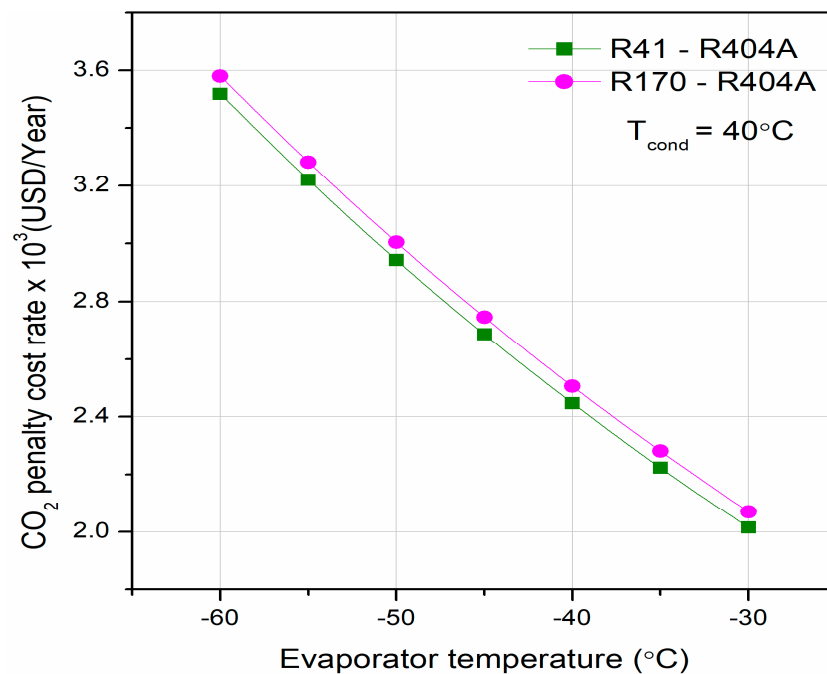

Figure 10. CO_2 penalty cost rate vs. T_{eva}.

It can also be noted from Figure 7 that the C_T of the system is slightly higher (about USD 200 per year) with refrigerant pair R170–R404A than with refrigerant pair R41–R404A throughout the investigated T_{eva} range, $-60\,°C$ to $-30\,°C$. Finally, a comparison between the exergy destruction and total annual plant cost rate is shown in Table 11.

Table 11. Variation of exergetic efficiency and annual plant cost rate with evaporator temperature.

Evaporator Temperature (°C)	Refrigerant Pair R170/R404A		Refrigerant Pair R41/R404A	
	Exergy Destruction (kW)	Total Plant Cost Rate (USD/Year)	Exergy Destruction (kW)	Total Plant Cost Rate (USD/Year)
−60	5.577	23001	5.425	22805
−55	5.1	22000	4.945	21798
−50	4.666	21108	4.511	20906
−45	4.27	20340	4.117	20139
−40	3.908	19725	3.758	19528
−35	3.576	19330	3.428	19131
−30	3.271	19332	3.127	19134

Table 11 shows that with the decrease in exergy loss the annual plant cost rate decreases. Both refrigerant pairs show a similar trend.

5. Conclusions

The following conclusions can be drawn from this thermoeconomic investigation into a CRS with a 10 kW cooling capacity.

- The COPs for both systems are comparable at any temperature.
- Refrigerant pair R170–R404A shows a 1.85% to 2.79% lower COP compared to refrigerant pair R41–R404A.
- The compressor discharge temperature is in favor of the system using refrigerant R170–R404A.
- The system with R170–R404A shows a 1.5% to 2.4% lower exergetic efficiency than the other system within the investigated evaporator temperature range.
- The total annual plant cost rate of the R170–R404A system is only USD 200 higher compared to that of the R41–R404A system.

Finally, it can be concluded that the system using refrigerant R170 can be a possible alternative to refrigerant R41 in the low-temperature cycle of the CRS, as R170 belongs to the hydrocarbon category and has lower GWP and zero ODP.

References

1. Coulomb, D.; Dupont, J.L.; Pichard, A. *The Role of Refrigeration in the Global Economy, 29th Informatory Note on Refrigeration Technologies*; International Institute of Refrigeration: Paris, France, 2015.
2. Heath, E.A. Amendment to the Montreal protocol on substances that deplete the ozone layer (Kigali amendment). *Int. Leg. Mater.* **2017**, *56*, 193–205. [CrossRef]
3. Lee, T.S.; Liu, C.H.; Chen, T.W. Thermodynamic analysis of optimal condensing temperature of cascade-condenser in CO_2/NH_3 cascade refrigeration systems. *Int. J. Refrig.* **2006**, *29*, 1100–1108. [CrossRef]
4. Hoşöz, M. Performance comparison of single-stage and cascade refrigeration systems using R134a as the working fluid. *Turk. J. Eng. Environ. Sci.* **2005**, *29*, 285–296.
5. Di Nicola, G.; Giuliani, G.; Polonara, F.; Stryjek, R. Blends of carbon dioxide and HFCs as working fluids for the low-temperature circuit in cascade refrigerating systems. *Int. J. Refrig.* **2005**, *28*, 130–140. [CrossRef]

6.   Niu, B.; Zhang, Y. Experimental study of the refrigeration cycle performance for the R744/R290 mixtures. *Int. J. Refrig.*
      2007, *30*, 37–42. [CrossRef]
7.   Ouadha, A.; En-Nacer, M.; Adjlout, L.; Imine, O. Exergy analysis of a two-stage refrigeration cycle using two natural substitutes
      of HCFC22. *Int. J. Exergy* **2005**, *2*, 14–30. [CrossRef]
8.   Sun, Z.; Liang, Y.; Liu, S.; Ji, W.; Zang, R.; Liang, R.; Guo, Z. Comparative analysis of thermodynamic performance of a cascade
      refrigeration system for refrigerant couples R41/R404A and R23/R404A. *Appl. Energy* **2016**, *184*, 19–25. [CrossRef]
9.   Dopazo, J.A.; Fernández-Seara, J. Experimental evaluation of a cascade refrigeration system prototype with CO_2 and NH_3 for
      freezing process applications. *Int. J. Refrig.* **2011**, *34*, 257–267. [CrossRef]
10.   Dopazo, J.A.; Fernández-Seara, J.; Sieres, J.; Uhı, F.J. Theoretical analysis of a CO_2–NH_3 cascade refrigeration system for cooling
      applications at low temperatures. *Appl. Therm. Eng.* **2009**, *29*, 1577–1583. [CrossRef]
11.   Rezayan, O.; Behbahaninia, A. Thermoeconomic optimization and exergy analysis of CO_2/NH_3 cascade refrigeration systems.
      Energy **2011**, *36*, 888–895. [CrossRef]
12.   Colorado, D.; Hernandez, J.A.; Rivera, W. Comparative study of a cascade cycle for simultaneous refrigeration and heating
      operating with ammonia, R134a, butane, propane, and CO_2 as working fluids. *Int. J. Sustain. Energy* **2012**, *31*, 365–381. [CrossRef]
13.   Messineo, A.; Panno, D. Performance evaluation of cascade refrigeration systems using different refrigerants. *Int. J. Air-Cond.
      Refrig.* **2012**, *20*, 1250010. [CrossRef]
14.   Aminyavari, M.; Najafi, B.; Shirazi, A.; Rinaldi, F. Exergetic, economic and environmental (3E) analyses, and multi-objective
      optimization of a CO_2/NH3 cascade refrigeration system. *Appl. Therm. Eng.* **2014**, *65*, 42–50. [CrossRef]
15.   Ust, Y.; Karakurt, A.S. Analysis of a Cascade Refrigeration System (CRS) by Using Different Refrigerant Couples Based on the
      Exergetic Performance Coefficient (EPC) Criterion. *Arab. J. Sci. Eng.* **2014**, *39*, 8147–8156. [CrossRef]
16.   Kasi, M.P. Simulation of thermodynamic analysis of cascade refrigeration system with alternative refrigerants. *Int. J. Mech. Eng.
      Technol. (IJMET)* **2015**, *6*, 71–91.
17.   Rawat, K.S.; Pratihar, A.K. Thermodynamic Analysis and Optimization of N_2O-NH_3 Cascade System for Low Temperature
      Refrigeration. *Int. J. Sci. Eng. Res.* **2017**, *7*, 150–154.
18.   Gholamian, E.; Hanafizadeh, P.; Ahmadi, P. Advanced exergy analysis of a carbon dioxide ammonia cascade refrigeration system.
      Appl. Therm. Eng. **2018**, *137*, 689–699. [CrossRef]
19.   Patel, V.; Panchal, D.; Prajapati, A.; Mudgal, A.; Davies, P. An efficient optimization and comparative analysis of cascade
      refrigeration system using NH_3/CO_2 and C_3H8/CO_2 refrigerant pairs. *Int. J. Refrig.* **2019**, *102*, 62–76. [CrossRef]
20.   Roy, R.; Mandal, B.K. Energetic and exergetic performance comparison of cascade refrigeration system using R170–R161 and
      R41–R404A as refrigerant pairs. *Heat Mass Transf.* **2019**, *55*, 723–731. [CrossRef]
21.   Adebayo, V.; Abid, M.; Adedeji, M.; Dagbasi, M.; Bamisile, O. Comparative thermodynamic performance analysis of a cascade
      refrigeration system with new refrigerants paired with CO_2. *Appl. Therm. Eng.* **2020**, *177*, 116286. [CrossRef]
22.   Aktemur, C.; Öztürk, İ.T. Energy and exergy analysis of a subcritical cascade refrigeration system with internal heat exchangers
      using environmentally-friendly refrigerants. *J. Energy Resour. Technol.* **2020**, *142*, 042009. [CrossRef]
23.   Aktemur, C.; Öztürk, İ.T.; Cimsit, C. Comparative energy and exergy analysis of a subcritical cascade refrigeration system using
      low global warming potential refrigerants. *Appl. Therm. Eng.* **2020**, *177*, 116254. [CrossRef]
24.   Zhang, Y.; He, Y.; Wang, Y.; Wu, X.; Jia, M.; Gong, Y. Experimental investigation of the performance of an R1270/CO_2 cascade
      refrigerant system. *Int. J. Refrig.* **2020**, *114*, 175–180. [CrossRef]
25.   Chen, X.; Yang, Q.; Chi, W.; Zhao, Y.; Liu, G.; Li, L. Energy and exergy analysis of NH_3/CO_2 cascade refrigeration system with sub
      cooling in the low-temperature cycle based on an auxiliary loop of NH_3 refrigerants. *Energy Rep.* **2022**, *8*, 1757–1767. [CrossRef]
26.   Sun, Z.; Wang, Y. Comprehensive performance analysis of cascade refrigeration system with two-stage compression for industrial
      refrigeration. *Case Stud. Therm. Eng.* **2022**, *39*, 102400. [CrossRef]
27.   Faruque, M.W.; Uddin, M.R.; Salehin, S.; Ehsan, M.M. A comprehensive thermodynamic assessment of cascade refrigeration
      system utilizing low GWP hydrocarbon refrigerants. *Int. J. Thermofluids* **2022**, *15*, 100177. [CrossRef]
28.   Cabello, R.; Andreu-Nácher, A.; Sánchez, D.; Llopis, R.; Vidan-Falomir, F. Energy comparison based on experimental results of a
      cascade refrigeration system pairing R744 with R134a, R1234ze(E) and the natural refrigerants R290, R1270, R600a. *Int. J. Refrig.*
      2023, *148*, 131–142. [CrossRef]
29.   Deymi-Dashtebayaz, M.; Sulin, A.; Ryabova, T.; Sankina, I.; Farahnak, M.; Nazeri, R. Energy, exergoeconomic and environmental
      optimization of a cascade refrigeration system using different low GWP refrigerants. *J. Environ. Chem. Eng.* **2021**, *9*, 106473.
      [CrossRef]
30.   Soni, S.; Mishra, P.; Maheshwari, G.; Verma, D.S. Theoretical energy analysis of Cascade refrigeration system using low Global
      warming potential refrigerants. *Mater. Today* **2022**, *63*, 164–169. [CrossRef]
31.   Klein, S.; Alvarado, F. *EES-Engineering Equation Solver: User's Manual for Microsoft Windows Operating Systems*; F-Chart Software:
      Madison, WI, USA, 2015.
32.   Calm, J.M.; Hourahan, G.C. Refrigerant Data Summary. *Eng. Syst.* **2001**, *18*, 74–77.
33.   Roy, R.; Mandal, B.K. Thermodynamic analysis of modified vapour compression refrigeration system using R-134a. *Energy
      Procedia* **2017**, *109*, 227–234. [CrossRef]
34.   Arora, A.; Kaushik, S.C. Theoretical analysis of a vapour compression refrigeration system with R502, R404A and R507A. *Int. J.
      Refrig.* **2008**, *31*, 998–1005. [CrossRef]

35. Mosaffa, A.H.; Farshi, L.G. Exergoeconomic and environmental analyses of an air conditioning system using thermal energy storage. *Appl. Energy* **2016**, *162*, 515–526. [CrossRef]
36. Sanaye, S.; Shirazi, A. Four E analysis and multi-objective optimization of an ice thermal energy storage for air-conditioning applications. *Int. J. Refrig.* **2013**, *36*, 828–841. [CrossRef]
37. Roy, R.; Bhowal, A.J.; Mandal, B.K. Exergy and cost optimization of a two-stage refrigeration system using refrigerant R32 and R410A. *J. Therm. Sci. Eng. Appl.* **2020**, *12*, 031024. [CrossRef]
38. Mosaffa, A.H.; Farshi, L.G.; Ferreira, C.A.I.; Rosen, M.A. Exergoeconomic and environmental analyses of CO_2/NH_3 cascade refrigeration systems equipped with different types of flash tank intercoolers. *Energy Convers. Manag.* **2016**, *117*, 442–453. [CrossRef]
39. Wang, J.; Zhai, Z.J.; Jing, Y.; Zhang, C. Particle swarm optimization for redundant building cooling heating and power system. *Appl. Energy* **2010**, *87*, 3668–3679. [CrossRef]
40. Chowdhury, S.; Roy, R.; Mandal, B.K. A review on energy and exergy analysis of two-Stage vapour compression refrigeration system. *Int. J. Air-Cond. Refrig.* **2019**, *27*, 1930001. [CrossRef]
41. Roy, R.; Mandal, B.K. Thermo-economic analysis and multi-objective optimization of vapour cascade refrigeration system using different refrigerant combinations: A comparative study. *J. Therm. Anal. Calorim.* **2020**, *139*, 3247–3261. [CrossRef]
42. Dincer, I.; Rosen, M.A.; Ahmadi, P. *Optimization of Energy Systems*; John Wiley & Sons: Nashville, TN, USA, 2017.
43. Sawalha, S.; Suleymani, A.; Rogstam, J. CO_2 *in Supermarket Refrigeration*; CO_2 Project Report Phase I; KTH Energy Technology: Stockholm, Sweden, 2006.